

Performance Enhancement of Induction Motor Based on Three-Level T-Type Inverter Using DTC-SVM

Ismail M. Abbas^{*}, Raaed F. Hassan

Middle Technical University, Baghdad, Iraq

Abstract. Induction motors (IM) that are driven using the conventional direct torque control algorithm (DTC) suffer from vital drawbacks which are high ripples in the torque and flux. These ripples result due to the use of a look-up table and hysteresis comparators which causes variable switching frequency. Moreover, the use of a traditional two-level inverter leads to the production of low-quality voltage and current. The work presented in this paper proposed a modified control system to overcome these drawbacks. The proposed control system is based on the use of the space vector modulation-based DTC algorithm (DTC-SVM) for driving three-phase IM via a three-level T-Type inverter. The conventional DTC-SVM algorithm has been modified to match the work of the proposed inverter. The modification process was based on the mapping of the standard DTC-SVM algorithm in the space vector of the three-level inverter. The conventional and the modified control systems are implemented using MATLAB/Simulink package. The comparison of the standard and the modified DTC-SVM has been performed by simulation. Simulation results showed the superiority of the proposed algorithm in terms of reducing ripple in torque and flux and improving the quality of current and voltage supplied to the motor.

Keywords - Induction Motor, Direct Torque Control, DTC-SVM, 3-level T-type Inverter, 2-level inverter

1. INTRODUCTION

Induction motors are the major electrical machine used in manufacturing and further applications [1]. They are popular in comparison to other motors, such as DC motors, because of their low cost, reliability, and flexibility [2, 3]. Induction motors utilize more than two-thirds of all industrial electrical energy [4]. Important advances in materials, power electronics, and high-performance microcontrollers are being made all the time, even though the basics of IM functioning have been known since the turn of the century. [5, 6]. So with high-performance microcontrollers and advanced power electronics switches IM drives offer a competitive advantage over DC machines [7]. To comply with norms such as four-quadrant operation, little torque variation, and quick speed recovery during load disturbances, high-performance drivers are used. The field-oriented control (FOC) and the Direct Torque (DTC) control method are the two most prevalent control methods for induction motors. Due to its ease of use, the DTC control algorithm has become the standard for governing induction motors. [3, 5, 8] Takahashi proposed the DTC method in 1986; the basis of this technique does

^{*}Corresponding Author: bcc0001@mtu.edu.iq

not necessitate complex computations or conversions; It includes a look-up table and flux and torque estimators. [9, 10]. DTC, on the other hand, has some significant drawbacks. It has strong torque ripples, particularly at low switching frequencies, resulting in fluctuating switching frequency and difficulty managing flux and torque at low speeds[11]. To overcome these disadvantages and increase DTC performance, a variety of approaches have been proposed. The most extensively used method for improving DTC performance, known as DTC-SVM, is based on the principle of space vector modulation[12-14]. However, with the presence of two-level inverters, improved ways to increase direct torque control make no contribution enough to the process of improvement. The non-sinusoidal output voltage produced by the two-level inverters contains significant harmonics distortion, which reduces drive performance[15, 16]. The Multi-Level Inverter (MLI) is used instead of a conventional 2-level inverter to mitigate these drawbacks by permitting the inverter to operate at higher voltage ratings and decreasing the harmonic content of the output voltage and current waveforms.[17]. There are three common types of multi-level inverter topology the cascaded H-bridge (CHB)[18-20], Neutral Point Clamped (NPC)[21], and Flying Capacitor (FC)[22-24], the cascaded H bridge inverter is suited for photovoltaic (PV) systems. The inverter's restriction is the vast number of DC sources for the upper level. Neutral Point Clamped and Flying Capacitor inverters only utilize a single DC supply, but they still require several semiconductor components and incur significant conduction losses. [25]. Therefore, a three-level T-type inverter has been proposed Because it has the advantages of using a single DC source, fewer components, and reduced conduction losses[26, 27]. The purpose of this paper is to investigate the impact of employing the DTC-SVM on an induction motor. When comparing the use of a DTC-SVM with a 2-level inverter to the use of a DTC-SVM with a 3-level T-type inverter.

2. T-TYPE MULTILEVEL INVERTER

Fig.1 depicts the layout of a T-type inverter with three phases and three output levels..

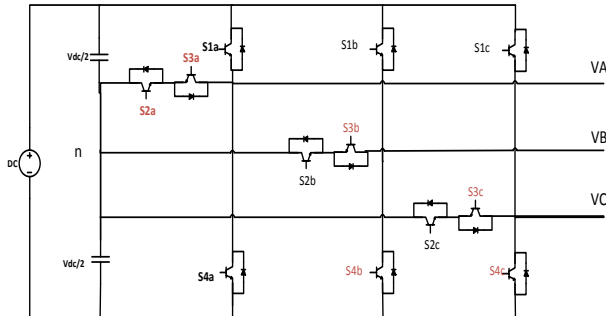


Fig.1. Configuration of 3-phase 3-Level T-type

An individual-leg, three-level T-type inverter's operating principles are discussed:

- When (S1a) ON and (S2a) ON be $V_a = V_{dc}/2$
 - When (S4a) ON and (S3a) ON be $V_a = -V_{dc}/2$
 - When (S2a) ON and (S3a) ON be $V_a = 0$
- as shown in Table I

TABLE I: Switching state of one arm 3-level T-type inverter

State	V _a	T1	T2	T3	T4
[P]	+V _{dc} /2	ON	ON	OFF	OFF
[O]	0	OFF	ON	ON	OFF
[N]	-V _{dc} /2	OFF	OFF	ON	ON

This construction is a 2-level inverter extension using a two-way switch attached to the midpoint n. This inverter's arms each have three switching states, resulting in three voltage levels. As a result, the three-phase three-level inverter will have 27 (3^3) switching states, and space vector's voltage vector count being increased, as illustrated in Fig.2. There are three kinds of voltage vectors (small vectors s1-s6, medium vectors m1-m6, and large vectors L1-L6). Furthermore, increasing the number of voltage vectors allows for an increase in the number of sectors that split the space vector, as seen in Fig.2. Table II shows how voltage vectors and their associated switching states are classified. There are 8 redundant switching states and 19 active switching states[28].

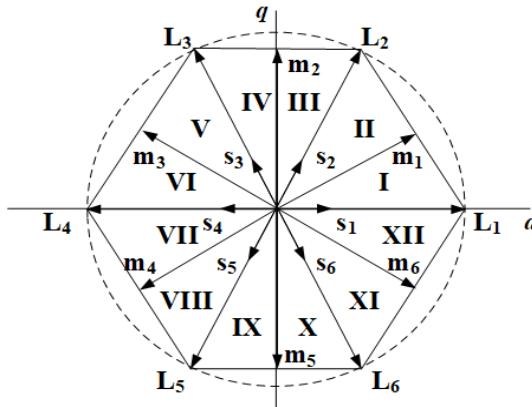


Fig.2. 3-Level T-type space vector

TABLE II. Three-level T-type switching states

Vector		Switching state
ZV	V0	[OOO],[PPP],[NNN]
SV	V1 – V6	[POO] or [ONN] [PPO] or [OON] [OPO] or [NON] [OPP] or [NOO] [OOP] or [NNO] [POP] or [ONO]
MV	V7 –V12	[PON] [OPN] [NPO] [NOP] [ONP] [PNO]
LV	V13 – V18	[PNN] [PPN] [NPN] [NPP] [NNP] [PNP]

3. DTC-SVM ALGORITHM

A major drawback of traditional DTC systems is the high frequencies and switching frequency. As a result, the augmented system will have high current harmonics, acoustic noise, and poor control performance, especially at low speeds. Because of the hysteresis comparator's discrete nature, high torque, flux ripples, and variable switching frequency remain significant even when the bandwidth is lowered.[29, 30]. Due to the comparatively small bandwidth values, the inverter switching frequency and switching losses are also

enhanced. To address these flaws, a group of researchers collaborated to combine the benefits DTC and FOC into a single framework, resulting in the novel DTC-SVM approach[31]. Unlike conventional DTC, which uses instantaneous values and direct computations to produce the inverter switching state, the DTC-SVM uses average values and the SVM algorithm to produce the inverter switching state[32]. The DTC-SVM technique is used to estimate the reference voltage vector, which is subsequently adjusted using the SVM technique to build inverter switches. The aim of this design is to regulate the flux and torque of an induction motor. In this method, the hysteresis control and the switching table are deleted, and instead, the proportional-integral (PI) controller and the SVM modulator are employed, as shown in Fig. 3.[8].

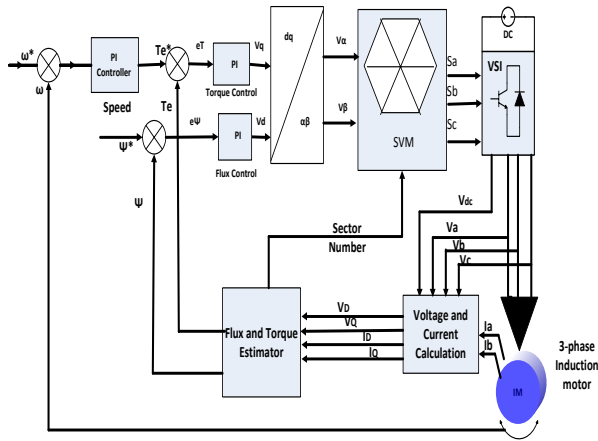


Fig. 3. DTC-SVM configuration.

A. DTC-SVM Algorithm for 2-Level Inverter

The two zero voltage vectors and six active space vectors formed in the two-level inverter are used to try and switch the space vector to fit the sinusoidal reference voltage. In order to bring the reference voltage vector V_s into phase with its neighboring vectors at the lowest switching frequency, the cycle T_s must be divided into three segments: T_a , T_b , and T_0 . The following on-time or volt-seconds computations can be conducted using the simplified geometry in Fig. 4.[31, 33]:

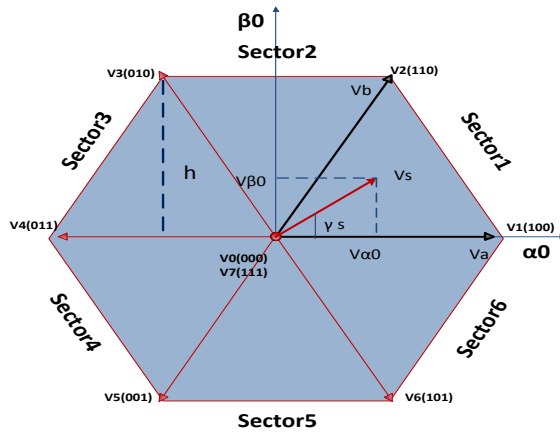


Fig. 4. Space vector of a 2-level inverter

$$\vec{V}_s T_s = T_a \vec{V}_a + T_b \vec{V}_b \tag{1}$$

In which $V_a = (1,0)$ and $V_b = (0.5h)$

$$T_a + T_b + T_0 = T_s \tag{2}$$

Taking the components of \vec{V}_s in quadrature axes yields:

$$V_{\alpha 0}^s T_s = t_a + 0.5t_b \tag{3}$$

$$V_{\beta 0}^s T_s = ht_b \tag{4}$$

From (5) to (7), the following are the on-time durations that can be determined:

$$T_a = T_s \left[V_{\alpha 0}^s - \frac{V_{\beta 0}^s}{2h} \right] \tag{5}$$

$$T_b = T_s \left[\frac{V_{\beta 0}^s}{h} \right] \tag{6}$$

The rest of the period will be:

$$T_0 = T_s - T_a - T_b \tag{7}$$

The resultant leg voltage for producing reference vectors in sector 1 is shown in Fig. 5. A circular path is formed by the sinusoidal reference space vector. The SVPWM produces the greatest significant output voltage at the radius of the largest circle that can fit inside the hexagon.

$$|\vec{V}_s^*| = \frac{2}{3} V_{dc} \cos\left(\frac{\pi}{6}\right) = \frac{1}{\sqrt{3}} V_{dc} \tag{8}$$

The DC bus voltage is denoted by V_{dc} . The following is the formula for calculating switching times (duty cycles)[34, 35].

$$T_{aon} = \frac{T_s - T1 - T2}{2} \tag{9}$$

$$T_{bon} = T_{aon} + T1 \tag{10}$$

$$T_{con} = T_{bon} + T2 \tag{11}$$

Table III shows the switching times (output) for each sector.

TABLE III. Switching times for each sector

Sector	1	2	3	4	5	6
Sa	Tbon	Taon	Taon	Tcon	Tbon	Tcon
Sb	Taon	Tcon	Tbon	Tbon	Tcon	Taon
Sc	Tcon	Tbon	Tcon	Taon	Taon	Tbon

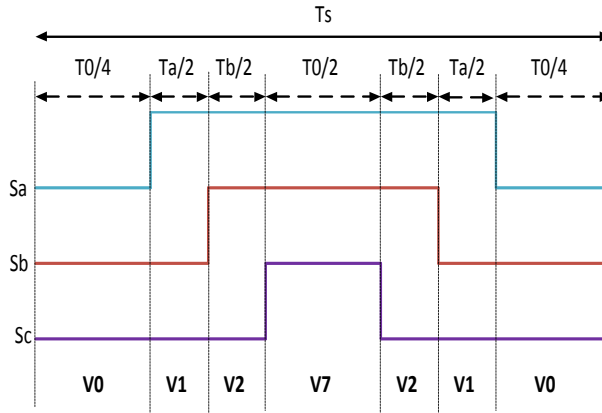


Fig. 5. Switching times of sector 1

B. DTC-SVM Algorithm for 3-Level T-type Inverter

Utilizing the identical arrangement, the DTC-SVM algorithm for controlling IM with a 3-level T-type inverter is built. According to Section II, the inverter contains eight redundant switching states in addition to 19 active switching states. The six sectors in Fig. 4 are divided so that each sector contains 4 triangles as in Fig. 6, the reference vector AOP of immensity $|V^*|$ is considered to reside in Δ_3 and creates an angle γ with the main axis α , extending the splitting of sector 1 into four triangles. As shown in Fig. 7 (a), (b) defining a little vector V^s in the Δ_3 , which defines point P. The needed volt-second for the AOP is the same as for the A2P. The vector A2P's on-time calculations are identical to the two-level inverter's on-time calculations at the specified sector. It is necessary to build the triangle into which the reference voltage vector is placed in a 3-level inverter, and the components of the small vector V^s ($V_{\alpha 0}^s$ and $V_{\beta 0}^s$) must be computed to determine the on-time required for every reference voltage vector. The on-time T_a , T_b , and T_0 values are calculated by (5)- (7)[33].

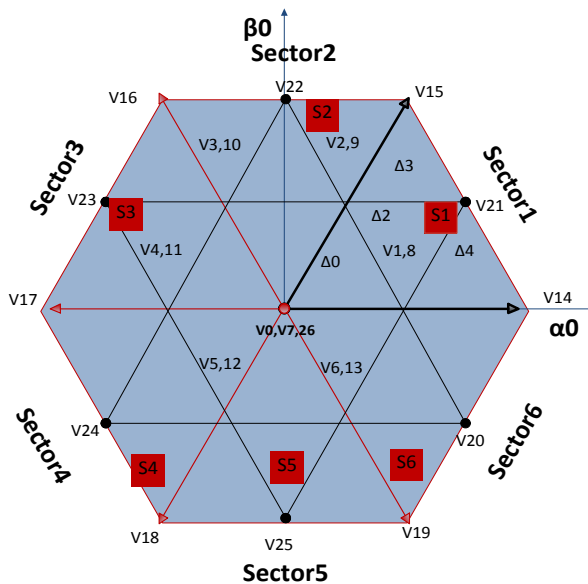


Fig. 6. Space vector of a 3-level T-type inverter.

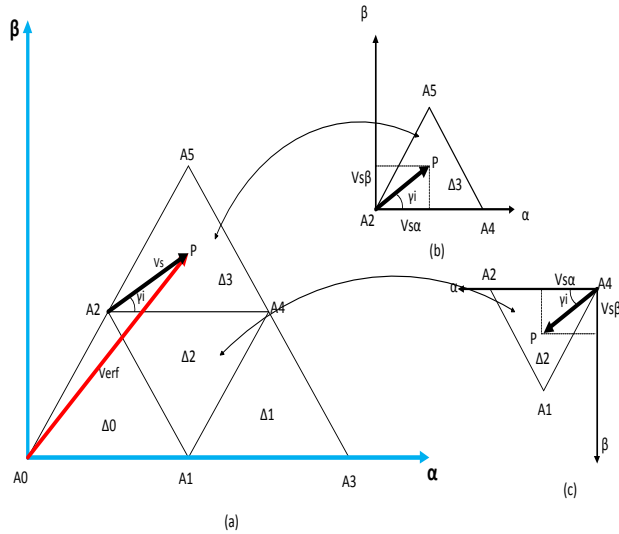


Fig. 7. Each sector is divided into four triangles.

The following is a summary of the technique for finding the on-time switching for a 3-level T-type inverter.

- Using the following equations, we can identify the sector S_i and γ within the sector for the desired reference vector:

$$S_i = \text{int}(\theta/60) + 1 \quad (12)$$

$$\gamma = \text{rem}(\theta/60) \quad (13)$$

- Define two integers to identify the $\Delta 1$ and the tiny vector v_s :

$$K_1 = \text{int} \left(V_\alpha + \frac{V_\beta}{\sqrt{3}} \right) \quad (14)$$

$$K_2 = \text{int} \left(\frac{V_\beta}{h} \right) \quad (15)$$

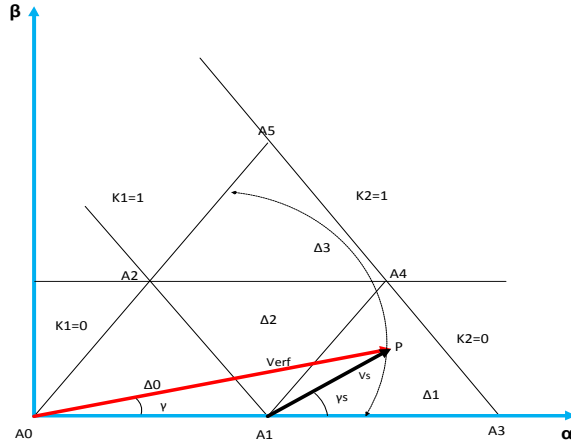


Fig. 8. Mapping of k_1 and k_2 in sector 1.

- Determine the components of the tiny vector v_s with relation to the virtual vertex (i.e., A_1 in Fig. 8):

$$V_{\alpha i} = V_{\alpha} - K_1 + 0.5K_2 \quad (16)$$

$$V_{\beta i} = V_{\beta} - K_2 h \quad (17)$$

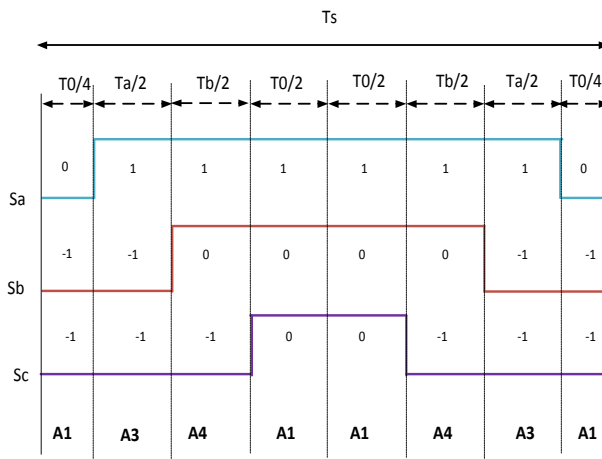


Fig. 9 Leg voltage for reference vector at sector 1, Δ_1 .

- To find the triangle number, do the following:

Where, $j = 0, 1,$ and 3

$$\Delta_j = K_1^2 + 2K_2 \quad (18)$$

Where, $j = 2$

$$\Delta_j = K_1^2 + 2K_2 + 1 \quad (19)$$

- Calculate the on-time switching based on (5) to (7).

A 3-level T-type inverter's switching waveforms are shown in Fig. 9.

4. SIMULINK IMPLEMENTATION

The DTC-SVM algorithm for a 2-Level inverter has been implemented using the MATLAB/Simulink program, as illustrated in Fig.10.

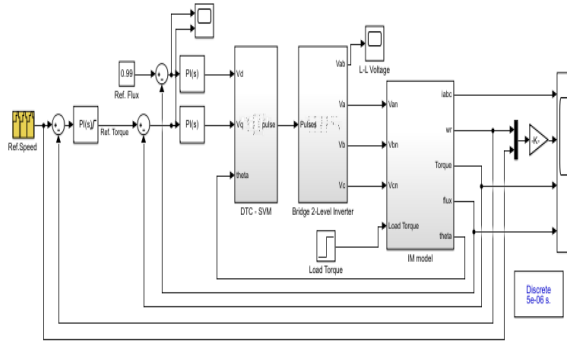


Fig.10 The DTC-SVM algorithm in Simulink

In this figure, and concerning Fig. 3, is the calculation of the switching times (output) for each sector, as shown in the equations (20-25) and Table IV.

Where: [x,y,z] = function (VAlpha,VBeta,Ts,Vdc) , Ts = Time constant

$$X = 1.732 * V\beta * Ts/Vdc \quad (20)$$

$$Y = 1.5 * (V\alpha + 0.577 * V\beta) * Ts/Vdc \quad (21)$$

$$Z = 1.5 * ((0.577 * V\beta - V\alpha) * Ts/Vdc) \quad (22)$$

Where: T1=0, T2=0

$$Ta = 0.25 * (Ts - T1 - T2) \quad (23)$$

$$Tb = 0.5 * T1 + Ta \quad (24)$$

$$Tc = 0.5 * T2 + Tb \quad (25)$$

Table IV. The calculation of the switching times (output) for each sector in Simulink(DTC-SVM)

Sector	ON Tim1	ON Tim2
1	T1 = Z T2 = Y	Sa = Tb Sb = Ta Sc = Tc
2	T1 = Y T2 = -X	Sa = Ta Sb = Tc Sc = Tb
3	T1 = -Z T2 = X	Sa = Ta Sb = Tb Sc = Tc

4	T1 = -X T2 = Z	Sa = Tc Sb = Tb Sc = Ta
5	T1 = X T2 = -Y	Sa = Tc Sb = Ta Sc = Tb
6	T1 = -Y T2 = -Z	Sa = Tb Sb = Tc Sc = Ta

The DTC-SVM algorithm for a 3-Level T-type inverter has been implemented using the MATLAB/Simulink program, as illustrated in Fig.11. In this figure, and concerning Fig. 8 and 9, is the calculation of the switching times (output) for each sector, as shown in the equations and Table V.

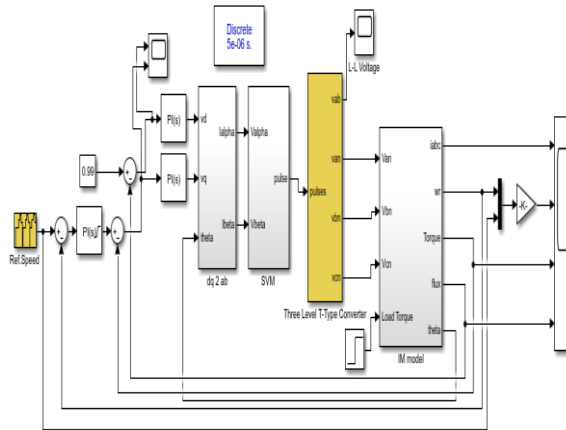


Fig. 11 The DTC-SVM algorithm for 3-level T-type inverter in Simulink
Calculating the on-time switching (T_a , T_b , and T_c) in the four triangles of fig. 9, as shown in the following equations:

$$T_a = T_s - 2K \sin \gamma \tag{33}$$

$$T_b = 2K \sin \left(\frac{\pi}{3} + \gamma \right) - T_s \tag{34}$$

$$T_c = T_s - 2K \sin \left(\frac{\pi}{3} - \gamma \right) \tag{35}$$

Where; $K = \frac{2}{\sqrt{3}} m_n T_s$, $m_n = \frac{v_{ref}}{2 * V_{dc} / 3}$

To get Y, where Y=Region as shown in Table IV.

Table V. Calculating the on-time switching (T_a , T_b , and T_c) in Region

On-Time Region	T_a	T_b	T_c
1	$2K \sin \left(\frac{\pi}{3} - \gamma \right)$	$T_s - 2K \sin \left(\frac{\pi}{3} + \gamma \right)$	$2K \sin \gamma$
2	$T_s - 2K \sin \gamma$	$2K \sin \left(\frac{\pi}{3} + \gamma \right) - T_s$	$T_s - 2K \sin \left(\frac{\pi}{3} - \gamma \right)$
3	$2K \sin \gamma - T_s$	$2K \sin \left(\frac{\pi}{3} - \gamma \right)$	$2T_s - 2K \sin \left(\frac{\pi}{3} + \gamma \right)$
4	$2T_s - 2K \sin \left(\frac{\pi}{3} + \gamma \right)$	$2K \sin \gamma$	$2K \sin \left(\frac{\pi}{3} - \gamma \right) - T_s$

In Table VI, to calculate the switching timings (output) for each sector, the Simulink (DTC-SVM) is used to drive the IM, which is based on a three-level T-type inverter.

Table VI. calculate the switching times (output) for each sector

Region Time	1	2	3	4
PWM-S1a	$\frac{T_c}{4} + \frac{T_a}{4}$	$\frac{T_c}{4} + \frac{T_a}{4} + \frac{T_b}{2}$	$\frac{T_s}{2} - \frac{T_c}{4}$	$\frac{T_s}{2} - \frac{T_a}{4}$
PWM-S2a	$\frac{T_s}{2}$	$\frac{T_s}{2}$	$\frac{T_s}{2}$	$\frac{T_s}{2}$
PWM-S1b	$\frac{T_c}{4}$	$\frac{T_c}{4}$	$\frac{T_c}{4} + \frac{T_a}{4}$	0
PWM-S2b	$\frac{T_s}{2} - \frac{T_a}{4}$	$\frac{T_s}{2} - \frac{T_a}{4}$	$\frac{T_s}{2}$	$\frac{T_a}{4} + \frac{T_b}{2}$
PWM-S1c	0	0	0	0
PWM-S2c	$\frac{T_s}{2} - \frac{T_a}{4} - \frac{T_c}{4}$	$\frac{T_c}{4} + \frac{T_a}{4}$	$\frac{T_c}{4}$	$\frac{T_a}{4}$

5. RESULTS OF SIMULATION

MATLAB/Simulink software is used to compare the performance of the IM utilizing the DTC-SVM algorithm for a 2-level inverter with the DTC-SVM algorithm for a 3-level T-type inverter. Table VII lists the simulation parameters for the control system.

TABLE VII. PARAMETERS OF SIMULATION

Parameter Name	Symbol	Value
Voltage DC	Vdc	250 V
Resistance to Stator Winding	Rs	1.85 Ω
Resistance to rotor winding	Rr	1.84 Ω
Impedance of the Stator Winding	Xls	64.09 Ω
Impedance of the rotor winding	Xlr	64.09 Ω
Impedance of Magnetization	Xm	60.32 Ω
The number of poles	P	4
Frequency	f	50 Hz
Inertia moment	J	0.007
Gain in proportion	Kp	8
Gain in integral	Ki	35
Limiter of torque	Tlim	25
Band of flux hysteresis	HBF	0.002
Band of torque hysteresis	HBT	0.04

Fig.12 depicts the behavior of the induction motor's torque and speed in response to their DTC-SVM algorithm reference value for a 2-level inverter. As demonstrated in Fig. 12(a), there is a notable ripple in the torque and as seen in Fig. 12(b), the speed maintains its reference value. Using the modified DTC-SVM algorithm for a 3-level T-type inverter, on the other hand, resulted in a noticeable improvement in IM performance, as shown in Fig. 13. The torque ripples in Fig. 13(a) are decreased, and the IM's speed responsiveness is improved, as illustrated in Fig. 13 (b).

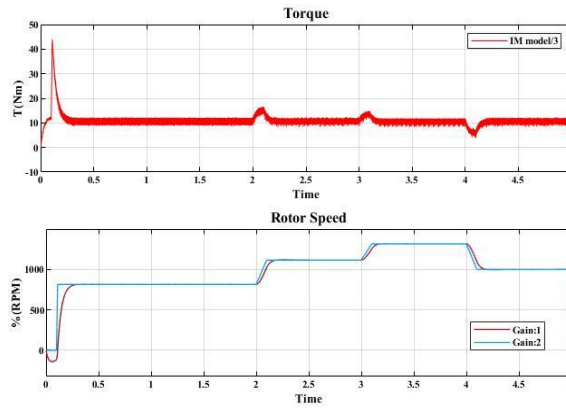


Fig. 12. IM behavior for DTC-SVM method for 2-level inverter; (a) torque reaction, (b) speed response

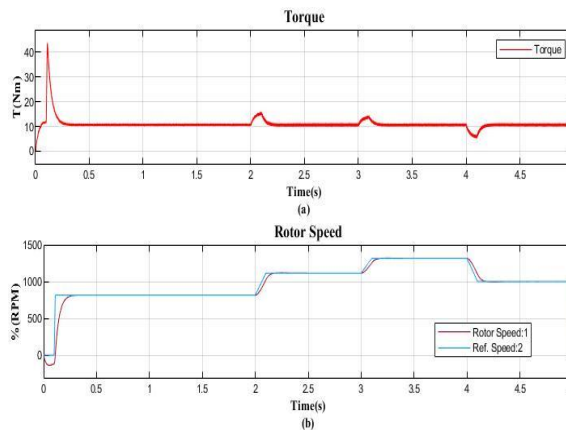


Fig. 13. IM behavior for DTC-SVM method for 3-level T-type inverter; (a) torque reaction, (b) speed response

Using a DTC-SVM with a 2-level inverter there are stator flux ripples as in Fig. 14 and they are significantly reduced when compared to using a DTC-SVM with a 3-level T-type inverter as in Fig. 15.

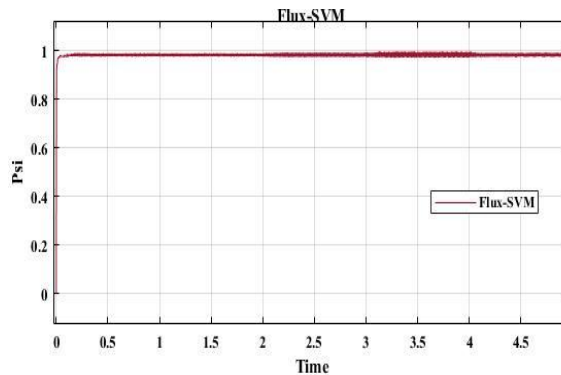


Fig.14 The DTC-SVM algorithm's stator flux locus for a 2-level inverter.

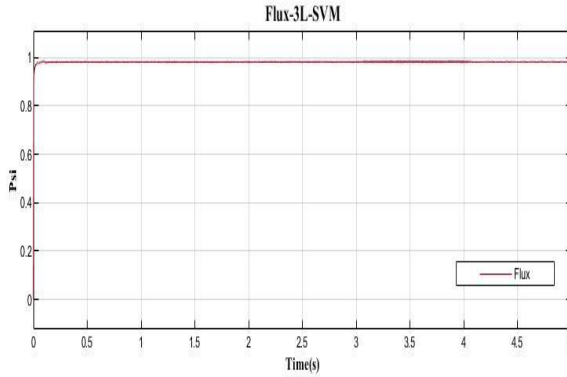


Fig.15 The DTC-SVM algorithm's stator flux locus for a 3-level T-type inverter. The quality of the stator currents greatly improves, when the DTC-SVM algorithm for a 3-level T-type inverter as shown in Fig. 16 is compared with the DTC-SVM algorithm for a 2-level inverter as shown in Fig. 17.

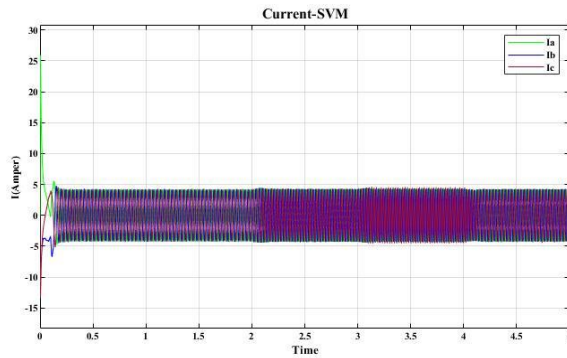


Fig. 16 Three-phase Stator Currents the DTC-SVM for 2-level inverter

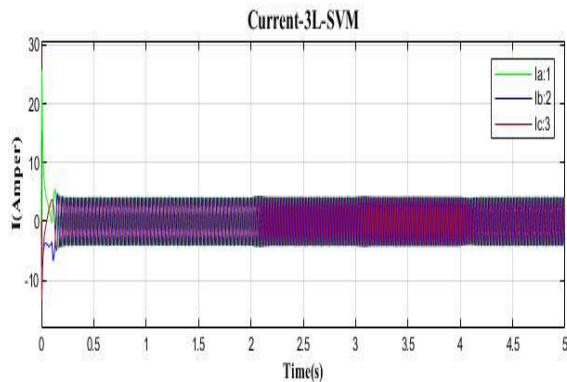


Fig. 17 Three-phase Stator Currents the DTC-SVM for 3-level T-type inverter

Fig. 18 shows the simulation results of the output voltage of the DTC-SVM for a 2-level inverter. And Fig. 19 shows the simulation results of the output voltage of the modified DTC-SVM

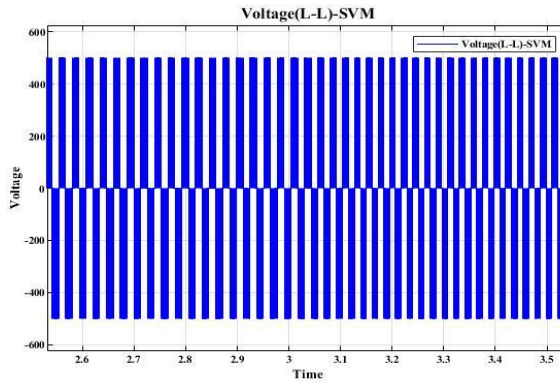


Fig. 18 the output voltage of the DTC-SVM for a 2-level inverter

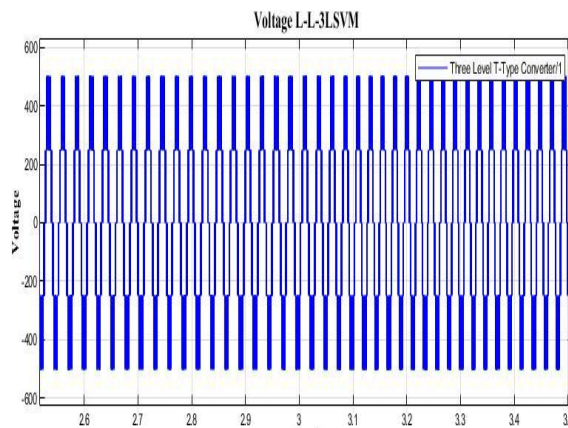
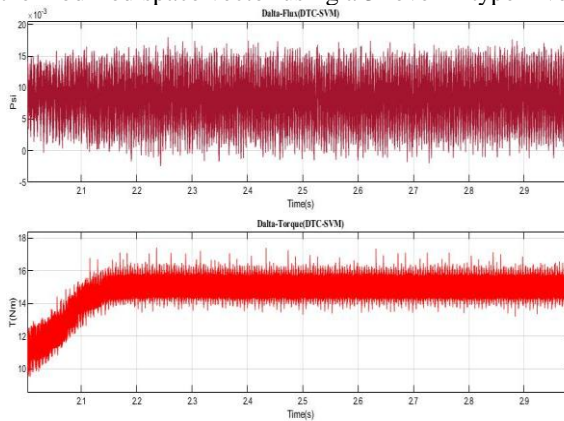


Fig. 19 the output voltage L-L of the DTC-SVM for a 3-level T-type inverter

Fig. 20 illustrates the comparison of IM performance based on the two control kinds systems provided in this paper, Fig. 20(b) space vector (DTC-SVM) with the 2-level inverter, comparing it with the modified space vector using a 3-level T-type inverter in Fig.20(b).



(a)

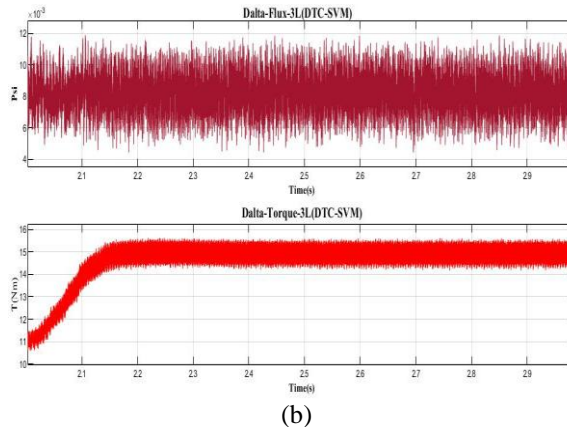


Fig.20 Examination of the induction motor's performance using two different controller types, (a) DTC-SVM with a 2-level inverter, and (b) DTC-SVM with a 3-level T-type inverter.

6. CONCLUSIONS

The influence of utilizing a multi-level inverter on the performance of the DTC-SVM to define the reference vector and switch-on-time is discussed in this paper, and it is compared to the DTC-SVM using a two-level inverter. The realized of employing a two-level inverter of DTC-SVM algorithms and a three-level T-type inverter of DTC-SVM algorithms to drive a three-phase IM using Matlab/Simulink. The DTC-SVM generated switching pulses as a function of space vector modulation. Although there are complex calculations as a result of the modification, the simulation results indicate a significant improvement in the performance of the induction motor

References

- [1] M. Hannan, J. A. Ali, A. Mohamed, A. J. R. Hussain, and S. E. Reviews, "Optimization techniques to enhance the performance of induction motor drives: A review," vol. 81, pp. 1611-1626, 2018.
- [2] M.-z. Niu, T. Wang, Q. Zhang, X. He, and M.-l. Zhao, "A new speed control method of induction motor," in *2016 35th Chinese Control Conference (CCC)*, 2016, pp. 10140-10143: IEEE.
- [3] A. A. Adam, Y. Haroen, A. Purwadi, and A. S. Rohman, "A study of a three phase induction motor performances controlled by indirect vector and predictive torque control," in *2018 5th International Conference on Electric Vehicular Technology (ICEVT)*, 2018, pp. 204-209: IEEE.
- [4] R. Dharmaprakash and J. J. M.-E. J. o. S. R. Henry, "Comparison of direct torque control of induction motor using two-level and three-level inverter," vol. 23, 2015.
- [5] M. A. Hannan, J. Abd Ali, P. J. Ker, A. Mohamed, M. S. Lipu, and A. J. I. a. Hussain, "Switching techniques and intelligent controllers for induction motor drive: Issues and recommendations," vol. 6, pp. 47489-47510, 2018.
- [6] S. Nayah and A. Khedher, "DTC of induction motor drives fed by two and three-level inverter: modeling and simulation," in *2019 19th International Conference on Sciences and Techniques of Automatic Control and Computer Engineering (STA)*, 2019, pp. 376-381: IEEE.
- [7] B. V. J. M.-E. j. o. s. r. Krishna, "Design and comparison of vector and direct torque control of 3-phase induction motor drive," vol. 20, no. 5, pp. 586-597, 2014.

- [8] A. J. Mohammed and R. F. Hassan, "Comparison of Conventional and Modified Direct Torque Control of Three-Phase Induction Motor Using Three-Level Flying Capacitor Inverter," *International Journal of Electrical and Electronic Engineering & Telecommunications*, vol. 10, 2021.
- [9] O. M. J. A. J. o. E. Meetei and E. Engineering, "Advanced control methods of induction motor: A review," vol. 1, no. 1, pp. 34-40, 2017.
- [10] O. Chandra Sekhar and S. J. I. T. o. E. E. S. Lakhimsetty, "Direct torque control scheme for a five-level multipoint clamped inverter fed induction motor drive using fractional-order PI controller," vol. 30, no. 9, p. e12474, 2020.
- [11] M. Vasudevan, R. Arumugam, S. J. E. c. Paramasivam, and management, "Real time implementation of viable torque and flux controllers and torque ripple minimization algorithm for induction motor drive," vol. 47, no. 11-12, pp. 1359-1371, 2006.
- [12] M. Pacas and J. J. I. t. o. i. e. Weber, "Predictive direct torque control for the PM synchronous machine," vol. 52, no. 5, pp. 1350-1356, 2005.
- [13] A. Tripathi, A. M. Khambadkone, and S. K. J. I. T. o. P. E. Panda, "Dynamic control of torque in overmodulation and in the field weakening region," vol. 21, no. 4, pp. 1091-1098, 2006.
- [14] A. J. Mohammed and R. F. Hassan, "DTC-SVM Control of Induction Motor Based on Dragonfly Optimization Algorithm," in *2022 Second International Conference on Advances in Electrical, Computing, Communication and Sustainable Technologies (ICAECT)*, 2022, pp. 1-8: IEEE.
- [15] S. El Daoudi, L. Lazrak, N. El Ouanjli, M. J. I. J. o. D. Ait Lafkih, and Control, "Improved DTC-SPWM strategy of induction motor by using five-level POD-PWM inverter and MRASSF estimator," vol. 9, no. 2, pp. 448-462, 2021.
- [16] S. El Daoudi, L. Lazrak, and M. A. Lafkih, "Modified direct torque control for sensorless asynchronous motor fed by three-level inverter," in *2020 1st International Conference on Innovative Research in Applied Science, Engineering and Technology (IRASET)*, 2020, pp. 1-4: IEEE.
- [17] P. M. Bhagwat and V. J. I. T. o. I. A. Stefanovic, "Generalized structure of a multilevel PWM inverter," no. 6, pp. 1057-1069, 1983.
- [18] M. Malinowski, K. Gopakumar, J. Rodriguez, and M. A. J. I. T. o. i. e. Perez, "A survey on cascaded multilevel inverters," vol. 57, no. 7, pp. 2197-2206, 2009.
- [19] G. Schettino, V. Castiglia, P. Livreri, R. Miceli, F. Viola, and R. Rizzo, "Novel computational method for harmonic mitigation for three-phase five-level cascaded H-bridge inverter," in *2018 International Conference on Smart Grid (icSmartGrid)*, 2018, pp. 299-306: IEEE.
- [20] M. Keddar, M. L. Doumbia, M. Della, K. Belmokhtar, and A. J. I. J. o. R. E. R. Midoun, "Interconnection performance analysis of single phase neural network based NPC and CHB multilevel inverters for grid-connected PV systems," vol. 9, no. 3, pp. 1451-1461, 2019.
- [21] J. Rodriguez, S. Bernet, P. K. Steimer, and I. E. J. I. t. o. I. E. Lizama, "A survey on neutral-point-clamped inverters," vol. 57, no. 7, pp. 2219-2230, 2009.
- [22] J.-i. Itoh, R. Ishibashi, and K. Kusaka, "Control Method of Flying Capacitor Converter Operated in Discontinuous Current Mode for High Voltage Photovoltaic Cell," in *2018 International Conference on Smart Grid (icSmartGrid)*, 2018, pp. 214-219: IEEE.
- [23] J. Huang and K. A. J. I. T. o. p. e. Corzine, "Extended operation of flying capacitor multilevel inverters," vol. 21, no. 1, pp. 140-147, 2006.
- [24] R. F. Hassan, N. M. J. I. J. o. E. Yasin, and Technology, "Model predictive control based stacked asymmetric multilevel inverter driver," vol. 7, no. 4, pp. 3924-3929, 2018.

- [25] S. Majumdar *et al.*, "Comparative Study of Space Vector Pulse Width Modulation based T-Type Three-level Inverter," vol. 4, no. 2, pp. 1-5, 2016.
- [26] H. Shin, K. Lee, J. Choi, S. Seo, and J. Lee, "Power loss comparison with different PWM methods for 3L-NPC inverter and 3L-T type inverter," in *2014 International Power Electronics and Application Conference and Exposition*, 2014, pp. 1322-1327: IEEE.
- [27] M. Q. Kasim, R. F. Hassan, A. J. Humaidi, A. I. Abdulkareem, A. R. Nasser, and A. Alkhayyat, "Control Algorithm of Five-Level Asymmetric Stacked Converter Based on Xilinx System Generator," in *2021 IEEE 9th Conference on Systems, Process and Control (ICSPC 2021)*, 2021, pp. 174-179: IEEE.
- [28] I. M. Abbas and R. F. Hassan, "T-Type Multilevel Inverter based Performance Improvement of Induction Motor," in *2022 Second International Conference on Advances in Electrical, Computing, Communication and Sustainable Technologies (ICAECT)*, 2022, pp. 1-6: IEEE.
- [29] T. G. Habetler, F. Profumo, M. Pastorelli, and L. M. J. I. T. o. i. a. Tolbert, "Direct torque control of induction machines using space vector modulation," vol. 28, no. 5, pp. 1045-1053, 1992.
- [30] H. Hiba, H. Ali, and H. Othmen, "DTC-SVM control for three phase induction motors," in *2013 International Conference on Electrical Engineering and Software Applications*, 2013, pp. 1-7: IEEE.
- [31] N. El Ouanjli *et al.*, "Modern improvement techniques of direct torque control for induction motor drives-a review," vol. 4, no. 1, pp. 1-12, 2019.
- [32] S. A. A. Tarusan, A. Jidin, M. L. M. Jamil, K. A. Karim, T. J. I. J. o. P. E. Sutikno, and D. Systems, "A review of direct torque control development in various multilevel inverter applications," vol. 11, no. 3, p. 1675, 2020.
- [33] A. J. Mohammed and R. F. Hassan, "Comparison of Conventional and Modified Direct Torque Control of Three-Phase Induction Motor Using Three-Level Flying Capacitor Inverter," 2021.
- [34] A. Ammar, A. Benakcha, and A. J. i. j. o. h. e. Bourek, "Closed loop torque SVM-DTC based on robust super twisting speed controller for induction motor drive with efficiency optimization," vol. 42, no. 28, pp. 17940-17952, 2017.
- [35] Y. Zahraoui, M. Akherraz, and C. J. U. S. B. Fahassa, Series C, "Induction Motor DTC Performance Improvement By Reducing Torque Ripples in Low Speed," vol. 81, no. 3, pp. 249-260, 2019.